crystallization papers

Crystallization and preliminary X-ray crystallographic investigations on several thermostable forms of a *Bacillus subtilis* lipase

Eerappa Rajakumara, Priyamvada Acharya, Shoeb Ahmad, Vellaiah M. Shanmugam, Nalam M. Rao* and Rajan Sankaranarayanan*

Centre for Cellular and Molecular Biology, Uppal Road, Hyderabad 500 007, India

Correspondence e-mail: madhu@ccmb.res.in, sankar@ccmb.res.in

Bacillus subtilis lipase loses activity above pH 10.5 and below pH 6.0. However, at low pH, *i.e.* below pH 5.0, the lipase acquires remarkable thermostability. Activity was unaltered for 2 h at 323 K at pH 4.0–5.0, although at pH values above 7.0 the activity was lost rapidly within minutes. Circular-dichroism studies indicate significant changes in the tertiary structure of the lipase, whereas the secondary-structural content remained unaltered. To elucidate the structural basis of the enhanced thermostability, three different forms have been crystallized at low pH along with three crystal forms of two thermostable mutants obtained using a directed-evolution approach.

1. Introduction

Lipases (EC 3.1.1.3) are triglycerol ester hydrolases that catalyze the hydrolysis of ester bonds. All structurally known lipases are serine hydrolases and belong to the α/β-hydrolase superfamily (Ollis *et al.*, 1992; Nardini & Dijkstra, 1999). These lipases have a highly conserved catalytic triad consisting of Ser, Asp/Glu and His (Ollis *et al.*, 1992). They have widespread applications in the modification of fats, as additives in detergents and as bio-catalysts (Jaeger & Reetz, 1998; Jaeger *et al.*, 1999). Therefore, modifying or enhancing a given property of these lipases such as substrate specificity or thermostability is not only useful in increasing the repertoire of compounds they can act upon, but also in increasing the optimum temperature of the reaction. Most of our current understanding of thermostability is guided by comparative sequence and structural analysis of proteins from mesophilic and thermophilic organisms. However, the differences that occur between these organisms cannot be directly attributed to the enhancement of thermostability, since this may result from other differences including genetic drifts and other selection pressures (Kumar *et al.*, 2000). In this scenario, directed-evolution approaches present an elegant way in which a given property of a protein, including its thermostability, can be enhanced.

Bacillus subtilis extracellular lipase (Lip A) is encoded by the *lipA* gene and is one of the smallest lipases with a molecular weight of 19.4 kDa (Dartois *et al.*, 1992). Lip A lipase does not show interfacial activation in the presence of oil–water interfaces (Dartois *et al.*, 1992) and is a typical mesophilic enzyme, showing optimum activity at 308 K and pH 8.0. Lip A lipase activity varies between pH 7.0 and 10.0 (Dartois *et al.*, 1992; Lesuisse *et al.*, 1993), decreasing strongly above pH 10.5 or below pH 6.5. However, Lip A lipase exhibits remarkable thermostability at or below pH 5.0. The enzyme preheated at 328 K for 20 min at pH 4.0–5.0 retained almost 100% activity when assayed at pH 8.0, whereas when preheated at pH 10 it completely loses activity in 2 min. The ability of the protein to withstand high temperature decreases when the pH of preheating was increased from 4.0 to 10.0. Intrinsic fluorescence and circular-dichroism studies indicate significant tertiary structural changes at low pH, whereas the secondary-structural content remains the same.

Using directed-evolution approaches, several thermostable mutants of Lip A have been obtained. Two of the most thermostable mutants, with more than 90- and 270-fold enhancement in half-life, were obtained by only two and three point mutations, respectively. In order to elucidate the structural basis of thermostability of these mutants and to understand the unusual thermostability of the wild-type enzyme at low pH, we undertook the purification, crystallization and characterization of several forms of Lip A lipase.

2. Materials and methods

2.1. Expression and purification

Purification of the protein from the over-producing strain *B. subtilis* BCL1051 was carried out essentially as described previously (Acharya & Rao, 2003) with minor modifications. The purity of the protein was checked by 12% SDS–PAGE. The protein was >95% pure on a Coomassie-stained gel. Enzyme assays were performed using *p*-nitrophenyl acetate as described previously.

2.2. Crystallization and preliminary X-ray data

For crystallization at low pH, screens were designed with the program *E-tray* (http://etray.sourceforge.net/) using combinations of different PEGs, salts and buffer of pH range 4.0–5.0. Crystallization trials were conducted using the hanging-drop vapour-diffusion method with varying drop volumes of protein solution equilibrated against 750 µl of reservoir solution. All crystallization attempts were made at room temperature. The initial crystallization conditions were refined with fine variations of pH, ionic strength and precipitant concentration. Screens were prepared using different combinations of PEGs and additives.

Preliminary diffraction data were collected on an in-house MAR research MAR-345dtb image-plate detector with Cu $K\alpha$ X-rays generated by a Rigaku RU-H3R rotating-anode generator operated at 50 kV and 100 mA equipped with an Osmic mirror system. Prior to flash-freezing in a liquid-nitrogen stream at 100 K for data collection, low-pH A, low-pH B and low-pH C crystals were soaked in 10, 5 and 10% glycerol, respectively, along with the mother liquor for 90–120 s. The mutant forms grew under conditions from which they could be flash-cooled directly in the liquid-nitrogen stream. X-ray data were processed using *DENZO* (Otwinowski & Minor, 1997) and subsequent scaling and merging of intensities were carried out using *SCALEPACK* (Otwinowski & Minor, 1997).

3. Results

Crystals were obtained under different conditions at low pH and can be classified into three categories: low-pH A, low-pH B and low-pH C. All low-pH crystal drops, which contained equal volumes (3 µl) of protein (8.7 mg ml^{-1} in 10 mM sodium acetate pH 4.0 and 5 mM sodium sulfate), were equilibrated against 750 µl of reservoir solution. Rod-shaped low-pH A crystals were grown from 26%(w/v) PEG 4000, 50 mM sodium citrate pH 4.5 and 50 mM ammonium sulfate and had a length of 75 µm (Fig. 1a). Low-pH B crystals were obtained from 32%(w/v) PEG 6000, 100 mM sodium acetate pH 5.0 and 15 mM ammonium sulfate. These crystals grew larger than low-pH A crystals and were 0.3 mm in length (Fig. 1b). The low pH C crystals grew from 28% PEG 6000, 100 mM sodium acetate pH 5.0, 25 mM ammonium sulfate

and 50 mM cesium chloride to dimensions of $0.6 \times 0.2 \times 0.2$ mm (Fig. 1c).

Initial search for crystallization conditions for mutants using the wild-type conditions, 35% PEG 4000, 0.1 M ethanolamine pH 10.0, 20 mM sodium sulfate and 3 mM CdCl$_2$ or 10 mM ZnCl$_2$, were unsuccessful (Pouderoyen *et al.*, 2001). The mutant crystals were obtained from conditions which lacked CdCl$_2$ or ZnCl$_2$, which were essential for the crystallization of the wild-type lipase. However, the presence of *n*-octyl-β-D-glucoside as an additive with PEG 3350 was needed to obtain mutant crystals. The double mutant crystallized in two forms, classified as DM1 and DM2, whereas the triple mutant (TM) crystallized in only one form. Protein solutions for crystallization were prepared in a buffer containing 0.1 M

ethanolamine pH 9.5 and 10 mM sodium sulfate, with concentrations of 8.5, 7.6 and 5.5 mg ml^{-1} for DM1, DM2 and TM, respectively. DM1 crystals were obtained from a hanging drop containing 3 µl of protein solution and 3 µl 1%(w/v) *n*-octyl-β-D-glucoside along with 3 µl of a reservoir solution consisting of 35%(w/v) PEG 3350, 0.1 M ethanolamine pH 9.5 and 20.0 mM sodium sulfate (Fig. 1d). DM2 crystallized in 34% PEG 3350, 0.1 M ethanolamine pH 10.5, 17.5 mM sodium sulfate, 1% *n*-octyl-β-D-glucoside and the drop contained equal volumes of protein (3 µl) and reservoir solution (Fig. 1e). The TM crystals were grown from 33% PEG 3350, 0.1 M ethanolamine pH 9.5, 22.5 mM sodium sulfate, 0.8% *n*-octyl-β-D-glucoside; the drop contained 5 µl of protein and 3 µl of reser-
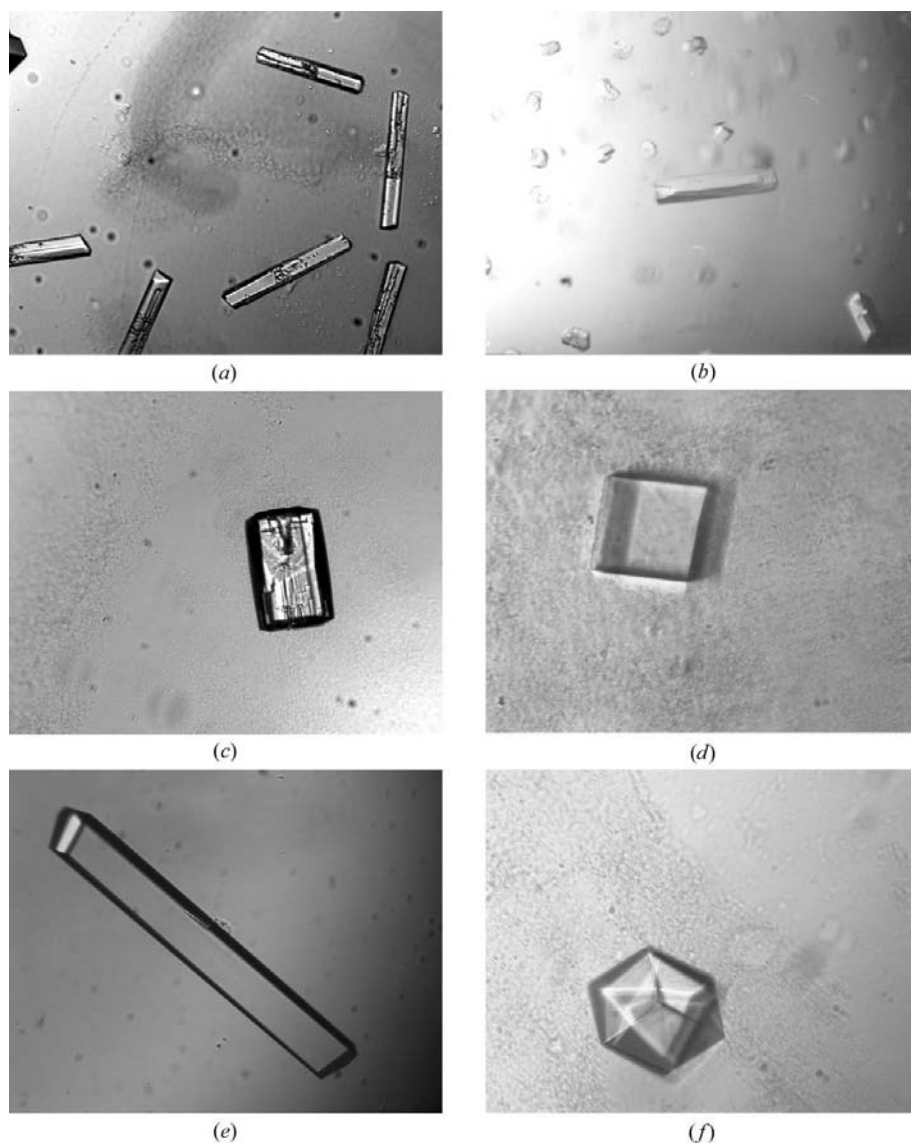

Figure 1
Different crystal forms of Lip A lipase: (*a*) tetragonal low-pH A, (*b*) orthorhombic low-pH B, (*c*) hexagonal low-pH C, (*d*) rhombohedral double mutant, (*e*) monoclinic double mutant and (*f*) rhombohedral triple mutant.

crystallization papers

Table 1
Essential crystallographic data.

Values in parentheses are for the highest resolution shell.

	Wild type			Mutant		
				Double mutant		Triple mutant
	Low-pH A	Low-pH B	Low-pH C	DM1	DM2	TM
Space group	$P4_22_12$	$P2_12_12$	Hexagonal	$R3$	$C2$	$R3$
Unit-cell parameters						
a (Å)	74.94	218.61	38.35	76.01	120.07	75.86
b (Å)		110.93			92.58	
c (Å)	112.02	52.00	350.49	103.93	79.96	102.67
β (°)					109.80	
Resolution (Å)	2.0 (2.07–2.0)	1.9 (1.97–1.90)		2.0 (2.07–2.0)	2.0 (2.07–2.0)	1.8 (1.86–1.8)
Observations	91125	306503		30111	69294	43884
Unique reflections	21687	96606		14097	37310	20293
Completeness (%)	97.7 (95.4)	95.9 (99.4)		94.2 (63.2)	88.9 (85.5)	99.3 (94.5)
Multiplicity	4.2 (4.0)	3.2 (3.6)		2.1 (1.9)	1.8 (1.8)	2.2 (2.0)
R_{merge}† (%)	10.6 (45.7)	9.5 (23.0)		4.4 (24.1)	10.1 (39.1)	2.6 (16.1)
$I/\sigma(I)$‡	11.1 (2.3)	11.8 (3.9)		19.0 (2.4)	8.3 (1.6)	32 (4.0)
Solvent content (%)	40.1	40.2		58.9	54.9	58.6
V_M (Å³ Da⁻¹)	2.1	2.1		3.0	2.7	3.0
Monomers per AU	2	8		1	4	1

† $R_{merge} = \sum |I(h) - \langle I(h)\rangle| / \sum I(h)$, where $I(h)$ is the observed intensity and $\langle I(h)\rangle$ is the mean intensity of reflection h over all measurements of $I(h)$.   ‡ Intensity signal-to-noise ratio.

voir solution (Fig. 1*f*). DM1 and TM were cubic in shape with a maximum dimension of 75–100 µm, whereas DM2 crystals were rod-shaped and grew up to 0.5 mm in length.

Low-pH A crystals diffract to 2.0 Å and belong to the tetragonal space group $P4_22_12$. The asymmetric unit contains two molecules, with a solvent content of 40%. Low-pH B crystals belong to the orthorhombic space group $P2_12_12$ and diffract to 1.90 Å resolution. Unit-cell volume calculations suggested the presence of eight molecules in the asymmetric unit, with a solvent content of 40%. The diffraction pattern from the low-pH C crystals could be indexed in the hexagonal system only after manual peak picking. However, all efforts to process the collected data and identify the space group were unsuccessful since the diffracted spots could not be resolved unambiguously using the in-house X-ray source, as one of the unit-cell parameters was around 350 Å. Low-pH crystal data statistics are shown in Table 1.

All the mutant crystal forms grown were different to that obtained for the wild-type enzyme (Ransac *et al.*, 1994; Pouderoyen *et al.*, 2001; Kawasaki *et al.*, 2002). DM1 and TM crystallized in a rhombohedral (*R*3) space group. DM1 and TM crystals diffracted to 1.8 and 2.0 Å resolution, respectively, and their asymmetric unit contained one molecule with a solvent content of 59%. Both the data sets were processed in the hexagonal *H*3 setting. DM2 crystallized in a monoclinic (*C*2) space group and diffracted to 2 Å resolution. It

contained four molecules in the asymmetric unit with a solvent content of 55%. The data-collection statistics of the mutant crystal forms are shown in Table 1.

Initial structure solution was attempted using the molecular-replacement method using the program *MOLREP-AUTO MR* (Vagin & Teplyakov, 1997) as implemented in the *CCP*4 suite (Collaborative Computational Project, Number 4, 1994). Two of the mutant crystal forms, DM1 and TM, readily yielded clear solutions in the rotational and translational search. The top solution gave correlation coefficients of 0.653 and 0.658, whereas the next solution gave correlation coefficients of 0.324 and 0.381 for DM1 and TM, respectively. The top solution gave *R* factors of 30.8 and 32.3 for DM1 and TM, respectively, after initial rigid-body refinement in *CNS* (Brünger *et al.*, 1998). Further analysis and refinement of the structures are in progress. The native Patterson maps using DM2 data indicated a pseudotranslation at (0, 0, 0.5); however, the rotational and translational molecular-replacement solutions could not be refined to a reasonable *R* factor.

Native Patterson maps of both the low-pH forms showed peaks that were more than 15% of the size of the origin peak. Low-pH A had a peak which is 82.2% of the origin peak and low-pH B had two peaks at 35.2 and 18.9% of the origin peak. This indicated the existence of pseudotranslation in both the crystal forms. An initial search using a monomer of the wild-type lipase (PDB code

1i6w) along with the pseudotranslation readily yielded a clear solution for the low-pH A crystal form. This solution could be refined to an *R* factor of 40.7% after initial rigid-body refinement. For the low-pH B form, the eight solutions expected from the unit-cell content analysis could not be obtained if the monomer is used as a search model. However, using a model consisting of two of the monomers, which were closely associated in the low-pH A crystal form, the other molecules in the asymmetric unit could be readily located. The eight monomers thus obtained gave an *R* factor of 36.4% after initial rigid-body refinement. Further refinement and analysis of these structures are in progress in order to understand the structural basis of unusual thermostability at low pH.

References

Acharya, P. & Rao, M. N. (2003). *J. Protein Chem.* **22**, 51–60.

Brünger, A. T., Adams, P. D., Clore, G. M., DeLano, W. L., Gros, P., Grosse-Kunstleve, R. W., Jiang, J.-S., Kuszewski, J., Nilges, M., Pannu, N. S., Read, R. J., Rice, L.M., Simonson, T. & Warren, G. L. (1998). *Acta Cryst.* D**54**, 905–921.

Collaborative Computational Project, Number 4 (1994). *Acta Cryst.* D**50**, 760–763.

Dartois, V., Baulard, A., Schanck, K. & Colson, C. (1992). *Biochim. Biophys. Acta*, **1131**, 253–260.

Jaeger, K. E., Dijkstra, B. W. & Reetz, M. T. (1999). *Annu. Rev. Miocrobiol.* **53**, 315–351.

Jaeger, K. E. & Reetz, M. T. (1998). *Trends Biotechnol.* **16**, 396–403.

Kawasaki, K., Kondo, H., Suzuki, M., Ohgiya, S. & Tsuda, S. (2002). *Acta Cryst.* D**58**, 1168–1174.

Kumar, S., Tsai, C.-J. & Nussinov, R. (2000). *Protein Eng.* **13**, 179–191.

Lesuisse, E., Schanck, K. & Colson, C. (1993). *Eur. J. Biochem.* **216**, 155–160.

Nardini, M. & Dijkstra, B. W. (1999). *Curr. Opin. Struct. Biol.* **9**, 732–737.

Ollis, D. L., Cheah, E., Cygler, M., Dijkstra, B., Frolow, F., Franken, S. M., Harel, M., Remington, S. J., Silman, I., Schrag, J., Sussman, J. L., Verschueren, K. H. G. & Goldman, A. (1992). *Protein Eng.* **5**, 197–211.

Otwinowski, Z. & Minor, W. (1997). *Methods Enzymol.* **276**, 307–326.

Pouderoyen, G. V., Eggert, T., Jaeger, K.-E. & Dijkstra, B. W. (2001). *J. Mol. Biol.* **309**, 215–226.

Ransac, S., Blaauw, M., Lesuisse, E., Schanck, K., Colson, C. & Dijkstra, B. W. (1994). *J. Mol. Biol.* **238**, 857–859.

Vagin, A. & Teplyakov, A. (1997). *J. Appl. Cryst.* **30**, 1022–1025.